



density, as Landau levels pass through the Fermi level, then there must be consequent changes in the potential profile across the structure in order to maintain a constant bias voltage. This results in a change in the wave function and energy of the bound state which in turn causes further changes in the Fermi energy, accumulated charge density, and potential profile. This feedback mechanism, activated by the change in external conditions, regulates the modifications in such a way that the 2DEG is always in a dynamic equilibrium state. The magneto-oscillations in the charge density, Fermi energy, and tunnel current must therefore be determined self-consistently. Some theoretical studies of the effect of a magnetic field on a 2DEG in modulation-doped or quantum-well structures have found a modulation of the charge density by the field.<sup>3,7-9</sup> But owing to the differences in device structures these results cannot be used to explain and analyze the experiments on  $n$ -type tunnel structures in which we are interested.

A full self-consistent numerical solution to the problem is computationally demanding as a self-consistent solution is required for each magnetic field and therefore is not suitable for the purpose of our present work, which is to elucidate the current modulation mechanism. In the present study, we have calculated the Fermi energy, charge density, tunnel current, and capacitance of the accumulated 2DEG as a function of magnetic fields using a variational method. With the variational approach we are able to explain and describe, using some simple physical arguments, the mechanism of the modulation of the charge density, Fermi level, and hence the tunnel current. In our model we only consider the Coulomb potentials of the accumulated 2DEG and the positive charges in the depletion layer. The effects of the bulk electrons and the background doping in the  $n^-$  layer, where the accumulated 2DEG is formed, are assumed to be negligible. We find that when the magnetic field is changed the Fermi energy and the charge density of the 2DEG both oscillate with the magnetic field. The tunnel current follows closely the oscillatory behavior observed experimentally. The current modulation is found to be the result of the charge-density modulation by the applied magnetic field. Some of the results have been reported in a conference<sup>10</sup> without a detailed discussion of the variational method. In this paper, we discuss the results and calculation in detail.

Several groups<sup>3,11-13</sup> have studied the magnetocapacitance of a 2DEG and obtain the density of states of the Landau levels. Some of these analyses assume that the charge distribution and the potential profile in the heterostructure remain unchanged during the measurement of the magnetocapacitance. However, as explained above, this assumption is not correct for a tunneling heterostructure, since, in the measurement of capacitance, the charges in the 2DEG and the potential profile are both changed by the change in the external bias voltage. There is a contribution to the capacitance due to the change in the potential profile. Our results show that the capacitance due to the change in potential profile is as important as the capacitance due to the density of states. It is necessary to take this effect into account in order to obtain quantitative information about the density of states of a 2DEG under a magnetic field.

This paper is organized in the following way. In Sec. II we will describe the structure of the device and review the

experimental results. The model and the calculation will be described in Sec. III. We discuss the theoretical results in Sec. IV and conclude the paper in Sec. V.

## II. REVIEW OF EXPERIMENTAL RESULTS

The single-barrier tunneling heterostructures which we consider consist of the following layers: a thick layer of heavily doped  $n^+$  semiconductor  $A$ ; a layer of lightly  $n^-$  doped semiconductor  $A$ ; a thin layer of undoped semiconductor  $B$ , with a larger band gap which acts as a barrier for the electrons; a thick layer of heavily doped  $n^+$  semiconductor,  $A$ . Metallic contacts are alloyed to the two heavily doped layers. The structure considered in our calculation has  $A = (\text{InGa})\text{As}$  and  $B = \text{InP}$ . The band structure (as seen by an electron at the conduction-band edge) of the device under an applied voltage is shown schematically in Fig. 1. On the left-hand side of the barrier is the  $n^-$  region, which is biased negatively with respect to the  $n^+$  region on the right-hand side so that a two-dimensional accumulation layer is formed at the interface between the  $n^-$  layer and the barrier. Because of a finite electric field in the barrier region, the shape of the barrier potential is not rectangular. A depletion layer, which gives rise to the band-bending  $\Delta V$ , is formed near to the interface between the barrier and the  $n^+$  layer. The potential drop of the device is mainly, across the barrier, the accumulation layer (in the  $n^-$  region), and the depletion layer in the  $n^+$  region.

At liquid-helium temperature, the current flowing through the device is mainly carried by electrons tunneling from the first subband of the accumulation layer. The electrons in the accumulation layer are degenerate and the applied voltage considered in the experiment is not high enough to create a second subband. Application of a magnetic field perpendicular to the barrier splits the density of states of the first subband into discrete Landau levels. When a fixed bias voltage is applied between the outer  $n^+$  contacts, the tunnel current oscillates as the magnetic field is swept. Eaves *et al.*<sup>1</sup> measured the magnetotunneling current of a  $\text{In}_x\text{Ga}_{1-x}\text{As}/\text{InP}$  tunneling heterostructure with structure parameters identical to those used in the present model calculation. They observe that the magnetic fields at which the current reaches a minimum are approximately given by  $B_f/n$ , where  $n$  is equal to 1, 2, 3, . . . , etc. Hickmott<sup>2</sup> studied the magnetotunneling current and the magnetocapacitance of  $\text{GaAs}/\text{Al}_x\text{Ga}_{1-x}\text{As}$  tunneling heterostructures. The barrier material in the heterostructures is  $\text{Al}_x\text{Ga}_{1-x}\text{As}$  ( $x=0.37, 0.4$ ) and the barrier thickness is 200 Å. He measured the oscillation of the tunnel current as a function of the magnetic field for various bias voltages. The current maxima and minima in the tunneling current are considered to be the result of the passage of the maxima and minima of the Landau-level density of states through the Fermi level. Both the analyses in Hickmott<sup>2</sup> and Eaves *et al.*<sup>1</sup> are based on some empirical models and do not consider the effects of changes in charge distribution with the magnetic field.

## III. MODEL

In order to understand the microscopic mechanism of the current modulation described in Sec. II, we have to perform

a variational calculation in which the bias voltage can be kept constant when the variational parameters and charge density are varied to minimize the energy. This facilitates comparison with experimental results which are obtained at fixed bias voltages when the magnetic field is changed. To reduce the complexity of the problem, we consider a simple model, in which the main physical features are retained. With this model, we can understand the magnetic-field modulation of the tunnel current and its relation to the electronic properties.

For the device which we consider here the tunnel barrier is sufficiently thick that the electrons in the accumulation layer have a long enough time to form a degenerate two-dimensional electron gas, which is almost in thermal equilibrium. The potential drop of the device is mainly across the barrier, the accumulation (in the  $n^-$  region) and the depletion (in the  $n^+$  region) layers. As the tunneling rate through the barrier is small in comparison with the scattering rates of electrons between the 2DEG states and the bulk states, the 2DEG is in equilibrium with the bulk electrons of the  $n^-$  layer and the device can be considered as a capacitor. Since the tunneling current in the heterostructure is small, the difference in Fermi levels between the  $n^-$  and the  $n^+$  layers on the left-hand side of the barrier is small and there is a constant Fermi level close to the conduction-band edge on the left of the barrier. Taking these factors into account, we make the following assumptions in our model:

(1) The main effect of the  $n^-$  region is to provide good electrical contact between the 2DEG and the external circuit so that the Fermi levels of the 2DEG and bulk electrons align with each other. The assumption of the pinning of the Fermi level is a major assumption of this model, which restricts the allowable range of the variational parameters and the shape of the wave function.

(2) To further simplify the calculation, We ignore the small difference in energy ( $\sim 4$  meV) between the conduction-band edge and the shallow-impurity levels.

(3) Only the first subband is occupied. The higher subbands are occupied only at high bias voltage ( $\sim 300$  mV). In this work we only consider the case in which one subband is occupied.

(4) The minority acceptors in the  $n^-$  region are ignored. In the  $n^-$  layer, there is always some background  $p$ -type doping, which can give rise to a space-charge layer and extra band bending. The amount of this background doping is not exactly known and depends on sample growth conditions. Ekenberg<sup>6</sup> has varied the amount of the fixed space charges to align the Fermi levels of the 2DEG and the bulk. The amount of the space charge is less than 10% of the 2DEG charge even for a large background doping. Since our interest is in understanding the effect of the magnetic field on the 2DEG, we ignore the background doping so as to simplify our calculation.

In an open system, like the 2DEG we are considering, exchange of particles with an external reservoir is allowed and equilibrium is established when the energy needed (gained) for putting (removing) a particle into (from) the 2DEG is equal to the work done by (to) the external voltage source. In the variational calculation we should minimize the grand potential  $\Omega$  of the 2DEG which is defined by

$$\Omega = U - NV_{\text{bias}}e, \quad (1)$$

where  $U$  is the sum of the kinetic and Coulomb interaction energies and  $N$  is the number density of the 2DEG. In a modulation-doped heterostructure, the Fermi level is uniform throughout the whole device, therefore only the total energy is minimized in the variational calculation.

In the discussion above, we have implicitly assumed that the electrons occupy bound states described by the variational wave function which has a zero expectation value for the current operator. This description does not seem to be appropriate for a tunneling device, as a realistic wave function should be nonzero throughout the barrier and connect with a traveling wave at the other side. One justification for this is that the tunneling current is very small and so is the traveling wave part of the wave function. Another justification is that in a ‘‘sequential’’ tunneling picture we can regard the variational wave function as the wave function of one of the two subsystems in the transfer Hamiltonian formalism.

The sequential picture of tunneling,<sup>14</sup> in which the process of tunneling is slower than the process of scattering into the accumulation layer, is also in accordance with the condition of equilibrium discussed above. When an electron tunnels into the  $n^+$  region, it loses its energy by inelastic scattering in the collector reservoir. The unoccupied state left behind is immediately filled by an electron ‘‘driven’’ into the accumulation layer by the external battery. Between two tunneling events the accumulation layer is constantly exchanging electrons with the reservoir on the left-hand side. If we average the total energy (as defined above) of the accumulation layer over a period of time which is longer than the inverse of the scattering rate but shorter than the inverse of the tunneling rate, the value does not exhibit any fluctuations due to scattering and is constant when the stationary state is established. It is quite clear from this consideration that this approach is only useful in the case of a thick and high barrier. In the case where the tunneling rate is comparable to the scattering rate, we cannot define a time scale on which the tunneling process is negligible and should include tunneling in the determination of the equilibrium configuration. This means that the variational approach is no longer valid.

We use the Fang-Howard<sup>15</sup> wave function in our variational calculation

$$\psi(z) = \begin{cases} \frac{2(z-as)}{a^{3/2}} e^{(z-sa)/a} & (z < as) \\ 0 & (z > as), \end{cases} \quad (2)$$

where  $z=0$  is the tunnel-barrier interface and  $a$  and  $s$  are variational parameters. For reasons explained below, two variational parameters are needed for the calculation. Parameter  $a$  has the dimension of length and is related to the spread of the charge in the direction perpendicular to the interface. Parameter  $s$  is a dimensionless parameter and is related to the penetration of the wavefunction into the barrier. The probability of finding the electron inside the barrier is equal to

$$\int_0^\infty |\psi(z)|^2 dz = u(s) = 1 - (2s^2 + 2s + 1)e^{-2s}. \quad (3)$$

We note that this wave function does not have an exponential tail in the barrier. However, the probability of finding the electron in the barrier is generally only a few percent so the linear approximation above is a sufficiently good approximation.

The depletion layer (which gives rise to the positive charge) in the  $n^+$  region has a finite thickness. For heavy doping, the thickness of the depletion layer is determined by the screening length. In our model, we simplify the calculation by assuming a very high doping so that the thickness of the depletion layer is negligible. As a result the band-bending  $\Delta V$  is negligible.

To determine the energy of the bound state in the accumulation layer, we first find the electric potential variation through the structure by solving Poisson's equation. We obtain the potential due to the positive ( $V_+(z)$ ) and negative ( $V_-(z)$ ) charges as

$$V_-(z) = \frac{eN}{\epsilon_r \epsilon_0} \left\{ -\frac{3}{4}a - \frac{1}{2}(z-sa) + \left[ \frac{(z-sa)^2}{a} - 2(z-sa) + \frac{3}{2}a \right] \exp\left(\frac{2(z-sa)}{a}\right) \right\} \quad (z > sa), \quad (4)$$

$$V_-(z) = \frac{eN}{\epsilon_r \epsilon_0} \left[ \frac{1}{2}(z-sa) + \frac{3}{4}a \right] \quad (z > sa), \quad (5)$$

$$V_+(z) = \frac{eN}{2\epsilon_r \epsilon_0} (z - 2b + sa - \frac{3}{2}a) \quad (z < b), \quad (6)$$

$$V_+(z) = -\frac{eN}{2\epsilon_r \epsilon_0} (z + \frac{3}{2}a - sa) \quad (z > b), \quad (7)$$

where the origin of potential is at  $z \rightarrow +\infty$  and the right-hand side of the barrier is at  $z = b$ .  $\epsilon_r$  is the relative dielectric constant of the material and  $N$  is the areal number density of electrons in the accumulation layer.

The asymptotic values of the total potential  $V(z) = V_+(z) + V_-(z)$  when  $z \rightarrow +\infty$  and  $z \rightarrow -\infty$  are given by

$$V(-\infty) = -\frac{eN}{\epsilon_r \epsilon_0} (b - sa + \frac{3}{2}a), \quad (8)$$

$$V(+\infty) = 0.$$

The potential difference across the sample,  $V(+\infty) - V(-\infty)$ , is related to the external bias  $V_{\text{bias}}$  by

$$V_{\text{bias}} = V(+\infty) - V(-\infty) - \frac{E_{\text{FR}}}{e} = \frac{eN}{\epsilon_r \epsilon_0} (b - sa + \frac{3}{2}a) - \frac{E_{\text{FR}}}{e}, \quad (9)$$

where  $E_{\text{FR}}$  is the Fermi energy of the bulk electrons in the right-hand  $n^+$  electrode. If we fix the external bias in this equation, we can determine one of the three variables ( $N, s, a$ ) as a function of the other two.

We now calculate the energy of the bound state  $E_B$ . This is given by the expectation values of the kinetic energy, the Coulomb potential energy  $V_+(z) + V_-(z)$ , and the

conduction-band discontinuity between the barrier and the  $n^-$  layer. In this order these terms give

$$E_B = \int_{-\infty}^{sa} \psi(z) \left( -\frac{\hbar^2}{2m_e} \frac{\partial^2}{\partial z^2} + V_+(z) + V_-(z) + V_B(z) \right) \psi(z) dz, \\ = \frac{\hbar^2}{2m_e a^2} - \frac{15e^2 Na}{32\epsilon_r \epsilon_0} + \frac{e^2 N}{\epsilon_r \epsilon_0} (\frac{3}{2}a - sa + b) + eV_b u(s), \quad (10)$$

where  $V_B(z)$  is the potential variation due to the conduction-band discontinuity and  $V_b$  is the conduction-band discontinuity between materials A and B.

The Fermi energy  $E_F$  of the 2DEG is equal to the energy difference between the bound-state energy and the Fermi level of the left contact, which is taken to be  $\mu_L = -eV(z \rightarrow -\infty)$ .

$$E_F = \mu_L - E_B = -\frac{\hbar^2}{2ma^2} - eV_b u(s) + \frac{15e^2 Na}{32\epsilon_r \epsilon_0}. \quad (11)$$

In the absence of a magnetic field the Fermi energy directly determines the number of electron per unit area by

$$N = E_F D_E, \quad (12)$$

where  $D_E$  is the density of states per unit area. Combining equations (9), (11), and (12), we can determine  $N$  and  $a$  as a function of the parameter  $s$ .

In a magnetic field, the density of states is not constant and we must write

$$N = \int_{-\infty}^{E_F} g(E) dE, \quad (13)$$

where  $g(E)$  is the density of states per unit area. We use a Gaussian-broadened density of states<sup>11,12</sup> given by

$$g(E) = xD_E + \sum_n \frac{2eB}{h} (1-x) \frac{1}{\Gamma \sqrt{\pi}} \\ \times \exp \left[ -\left( \frac{E - (n + \frac{1}{2})\hbar\omega_c}{\Gamma} \right)^2 \right], \quad (14)$$

where  $xD_E$  is the nonzero background density of states ( $x = 0.05$  in the present calculation),  $B$  is the magnetic field, and  $\Gamma$  is the broadening parameter which is related to the magnetic field by  $\Gamma_0 \sqrt{B}$ .  $\Gamma_0$  is chosen to be  $9 \times 10^{-4}$  eV  $\text{T}^{-1/2}$ . We have used different values of  $\Gamma_0$  and a different density of states and find that the details of the oscillatory structures in the theoretical results are modified. For example, when we increase the broadening, the amplitudes of the oscillations are reduced and the positions of the minima and the maxima are shifted slightly. This is important when a quantitative comparison is made between the theoretical and experimental results. As we have stated above, the main aim of this paper is to acquire an under-

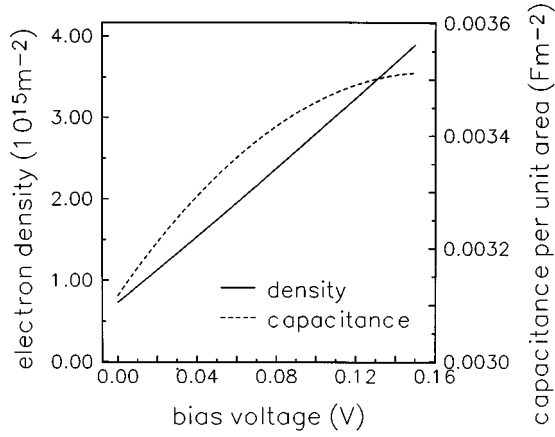


FIG. 2. The areal density and the differential capacitance per unit area of the accumulated electron plotted as a function of the applied voltage at zero magnetic field.

standing of the microscopic mechanisms. Thus the details of the broadening of the Landau levels do not have much bearing on the present work.

In this variational calculation, the grand potential  $\Omega$  is minimized by varying the parameters  $a$  and  $s$  subjecting to the constraint that the bias voltage is kept constant. The expression of the grand potential is given by

$$\Omega = \frac{N\hbar^2}{2m_e a^2} - \frac{15e^2 N^2 a}{64\epsilon_r \epsilon_0} + \frac{e^2 N^2}{2\epsilon_r \epsilon_0} \left(\frac{3}{2}a - sa + b\right) + eV_b u(s) + \int_{-\infty}^{E_F} g(E)E dE - eNV_{\text{bias}}. \quad (15)$$

In this expression the first and second terms are, respectively, the kinetic energy in the  $z$  direction and the potential energy due to the Coulomb interaction between the negative charges. The third term is the potential energy due to the interaction between the positive and the negative charges. The fourth term is the increase in energy due to the penetration of the wave function into the barrier. The fifth term is the energy of the motion in the  $x$ - $y$  plane. In a typical step of the numerical calculation, we first fix the bias voltage  $V_{\text{bias}}$  and an initial value of  $s$ . Electron density  $N$  and variational parameter  $a$  are then obtained by solving equations (9), (11), and (12) (at zero magnetic field). When there is a magnetic field, Eq. (12) should be replaced by Eq. (13). After  $N$  and  $a$  are determined, we then calculate the grand potential  $\Omega$ . The step is then repeated for other values of  $s$  so as to find the solution which minimizes the grand potential.

## IV. THEORETICAL RESULTS

### A. Results at zero magnetic field

It is interesting to know the properties of the 2DEG predicted by the present model at zero magnetic field. In Fig. 2 we plot the electron density and the differential capacitance per unit area  $\delta Q/\delta V$  as a function of the applied voltage at zero magnetic field. The tunneling heterostructure studied in this work has a barrier thickness of 200 Å, a barrier height of 200 meV, and a doping density of  $4 \times 10^{23} \text{ m}^{-3}$  in the  $n^+$  region on the right-hand side. The electron effective mass we

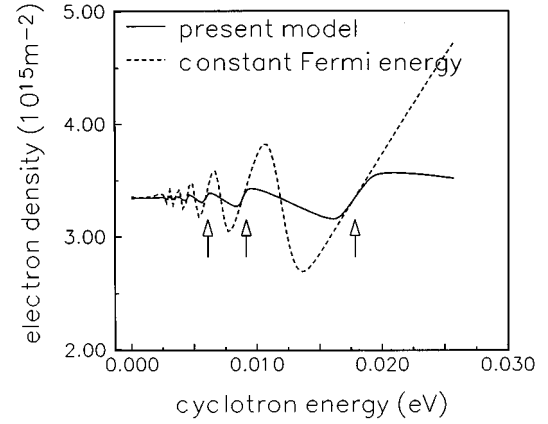


FIG. 3. The areal electron density of the accumulated electrons plotted as a function of the magnetic field at a fixed applied voltage of 0.125 V. The magnetic field is in the unit of cyclotron energy  $\hbar eB/m_e$ . Solid line is for the present model. Dashed line is obtained assuming a constant Fermi energy. The arrows show the positions for  $n\hbar\omega_c = E_F$ , where  $n=1,2,3$ .

used is  $0.045m_0$ . The relative dielectric constant is taken to be 12.5. We have ignored the differences between the material parameters of InP and In(Ga)As. Since the right-hand side of the barrier is doped, at zero-bias voltage the accumulation layer has a density of  $7.5 \times 10^{14} \text{ m}^{-2}$ . When the applied voltage is increased to 0.15 V, the accumulated electron density increases to  $3.8 \times 10^{15} \text{ m}^{-2}$ . The variational parameter  $a$  decreases with the applied voltage from 158 to 110 Å while the variational parameter  $s$  increases with the applied voltage from 0.1 to 0.2. For the voltages considered the penetration of the wave function (equal to  $sa$ ) into the tunneling barrier is not negligible. This effect reduces the electron's distance from the barrier by about 6–10%. The average distance of the electrons from the barrier  $\langle z \rangle$  is related to parameters  $a$  and  $s$  by  $\langle z \rangle = (1.5 - s)a$ . When the applied voltage is increased, the electrons are confined by a stronger electric field and as a result  $\langle z \rangle$  is reduced. In view of this, it is interesting to know whether the relation between electron charge and voltage is linear. In Fig. 2, the differential capacitance increases from  $3.1 \times 10^{-3} \text{ F m}^{-2}$  to  $3.5 \times 10^{-3} \text{ F m}^{-2}$  when the bias voltage is changed from 0 to 0.15 V. This nonlinearity is due to the decrease in the mean distance of the 2DEG charges from the barrier. Although the charge-voltage relation at zero magnetic field is not linear, it is a reasonable approximation to describe the charge-voltage relation with the ideal capacitor model, which gives an error of about 10%.

### B. Charge density and Fermi energy under an applied magnetic field

In Figs. 3 and 4 we plot the magnetic-field dependence of the electron density  $N$  and the Fermi energy of the 2DEG at an applied voltage of 0.125 V ( $E_F = \mu_L - E_B$ ), respectively. In these two figures, we also show the electron density calculated by assuming a constant Fermi energy and the Fermi energy calculated by assuming a constant electron density. These quantities oscillate with the magnetic field,  $B$ . When the applied voltage is increased, the oscillations shift to higher magnetic fields. Instead of showing the oscillations

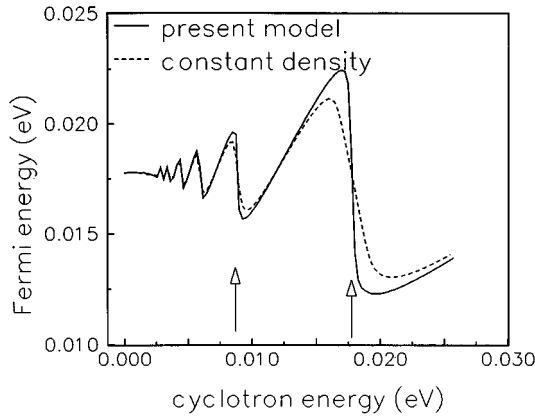


FIG. 4. The Fermi energy of the accumulated electron plotted as a function of the cyclotron energy. The solid line shows the results of the present model and the dashed line shows results assuming a constant areal density. The arrows show the positions for  $n\hbar\omega_c = E_F$ , where  $n = 1, 2$ .

for different applied voltages, we show only the results for a fixed applied voltage and discuss the mechanism of oscillation at a fixed bias. For an applied voltage of 125 mV, the electron density at zero magnetic field is about  $3.34 \times 10^{15} \text{ m}^{-2}$ , which corresponds to a Fermi energy of 17.8 meV. In Figs. 3 and 4, when we increase the magnetic field, both the Fermi energy of the 2DEG and the electron density oscillate symmetrically about the zero field value with opposite phases. It is clear that neither one of the following assumptions works: The total electron density is constant, or the Fermi energy of the 2DEG is constant. We notice the following distinctive features: (i) the Fermi energy of the 2DEG is a maximum when the electron density is a minimum and vice versa; (ii) the amplitudes of the magneto-oscillations in the 2DEG density and the Fermi energy are smaller than those amplitudes determined by assuming either a constant density or a constant Fermi energy. Below we shall discuss the physical mechanism of the modulation of these quantities by the magnetic field.

With a magnetic field we can modify the electron density by changing the density of states of each Landau level. When the Fermi level is near to the center of a Landau level  $[(n + 1/2)\hbar\omega_c = E_F]$ , i.e.,  $\hbar\omega_c \approx 36, 12, 7.2 \text{ meV}, \dots$  in Figs. 3 and 4] and there is a large density of states at the Fermi level, an increase in the magnetic field moves the Landau level upwards and forces a large number of charges out of the potential well. For a fixed bias voltage, this will increase the average distance of charges from the barrier [as predicted in Eq. (9)]. When the distance from the barrier increases, the Fermi energy of the 2DEG is increased as the bound-state energy is lowered. Therefore whenever the Fermi level is at a Landau level, any increase in the magnetic field will be accompanied with an increase in the Fermi energy. The increase in the Fermi energy is generally slower than the increase in the Landau-level energy and therefore the electron density gradually decreases. Because of this feedback mechanism and the change in the Fermi energy, the electron density decreases with a rate less than that predicted by assuming a constant Fermi energy. When the Fermi level is at a gap between two Landau levels ( $n\hbar\omega_c = E_F$ , i.e.,  $\hbar\omega_c = 18, 9 \text{ meV}, \dots$  in Figs. 3 and 4) and the density of

states is zero or at a minimum, the change in the number of electrons is determined by the change in the total number of states by the magnetic field. When there is an increase in magnetic field, the total number of available energy states below the Fermi level is increased and hence the electron density is increased. This results in a decrease in the average distance from the barrier  $\langle z \rangle$ . The Fermi energy will be decreased as  $\langle z \rangle$  is decreased.

In summary, when there is a high density of states at the Fermi level (i.e., the Fermi level is close to a Landau level), the 2DEG's Fermi energy increases and the electron density decreases with an increase in magnetic field. When there is a small density of states at the Fermi level (i.e., the Fermi level is in between two Landau levels), the 2DEG's Fermi energy decreases and the electron density increases. When the magnetic field gradually increases from zero, the Fermi energy and the electron density oscillate with opposite phases about their zero-field values. The amplitudes of oscillation are smaller than those predicted by assuming either a constant electron density or a constant Fermi energy.

### C. Tunnel current under an applied magnetic field

In Sec. IV B, we have discussed using a simple model, the mechanism of oscillation of the Fermi energy, and the electron density when the applied magnetic field is changed. However, in experiments, we can only measure the tunnel current from the 2DEG. Therefore, to analyze measured results, it is necessary to relate the tunnel current to the electron density and the potential profile in the heterostructure. In a semiclassical picture the tunnel current is proportional to the product of the electron density, the transmission coefficient, and the rate at which a single electron confined in the potential well hits the barrier (the attempt rate). The latter quantity is equal to the average velocity of an electron ( $\hbar/\pi am$ ) divided by the width of the potential well (proportional to  $a$ ). The tunnel current is therefore proportional to the following expression:

$$\frac{Te\hbar N}{\pi a^2 m}, \quad (16)$$

where  $T$  is the transmission coefficient through the tunneling barrier. The variation in potential across the barrier is smooth and slow (linear in  $z$  due to the electric field) compared with the decay length of the electron wave function in the barrier so the WKB method will give a good approximation for the transmission coefficient as follows:

$$\begin{aligned} T &\propto \exp\left\{-2 \int_0^b \frac{2m}{\hbar^2} \left(-\frac{e^2 N}{\epsilon_r \epsilon_0} z + E_h\right)^{1/2} dz\right\} \\ &= \exp\left\{-\frac{4E_h^{3/2} \epsilon_r \epsilon_0 \sqrt{2m}}{3e^2 N \hbar} \left[1 - \left(1 - \frac{e^2 N}{E_h \epsilon_r \epsilon_0} b\right)^{3/2}\right]\right\}, \\ E_h &= eV_b - \frac{e^2 N (3-2s)a}{\epsilon_r \epsilon_0} - \frac{e^2 N b}{2\epsilon_r \epsilon_0} + E_F, \quad (17) \end{aligned}$$

where  $E_h$  is the energy difference between the bound state and the top of the energy barrier.

The tunnel current is proportional to both the electron density and the transmission coefficient, and is inversely pro-

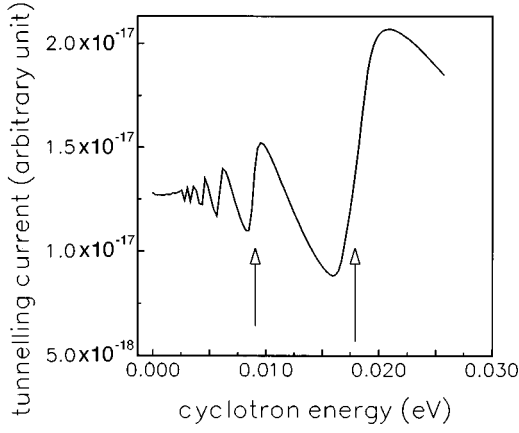


FIG. 5. The tunneling current (arbitrary unit) plotted as a function of the cyclotron energy. The arrows show the positions for  $n\hbar\omega_c = E_F$ , where  $n=1,2$ .

portional to the square of parameter  $a$ . Since  $a$  is approximately equal to  $2\langle z \rangle/3$ , the tunnel current can be regarded as inversely proportional to the square of the distance from the barrier. The current calculated using Eqs. (16) and (17) (shown in Fig. 5) follows closely the trend of these three factors. When the current is a maximum (minimum), the electron density is a maximum (minimum), the transmission coefficient (shown in Fig. 6) is a maximum (minimum) and the distance from barrier is a minimum (maximum). To understand how the transmission coefficient is modulated by the magnetic field, we plot the quantity  $E_h$  in Fig. 6 with the transmission coefficient. According to Eq. (17) the transmission coefficient is a function of  $E_h$  and  $N$ . If  $N$  is kept constant the transmission coefficient decreases with an increase in  $E_h$  as the effective barrier height is increased. However, in the present case, when  $E_h$  increases, the transmission coefficient increases. This shows that the change in the transmission coefficient is determined by the electron-density modulation. When the electron density is increased (decreased), there is a stronger (weaker) electric field at the tunneling barrier and hence a smaller (larger) transmission coefficient. In the present case, the oscillation in tunnel current is mainly due to the oscillation in charge density and the charges' distance from the barrier.

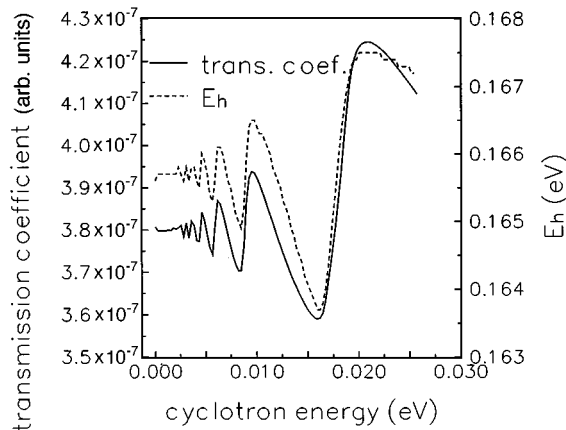


FIG. 6. The transmission coefficient (solid line) and  $E_h$  (dashed line) plotted as a function of the cyclotron energy.

TABLE I. Positions of current minima.

	Current minima obtained from Fig. 5	Current minima predicted by $E_F/(n+\phi)$ with $\phi=0.19$ and $E_F=17.8$ meV
$n=1$	14.87 meV	14.95 meV
$n=2$	8.26 meV	8.17 meV
$n=3$	5.58 meV	5.57 meV
$n=4$	4.13 meV	4.24 meV

In the analysis of Eaves *et al.*,<sup>1</sup> the tunneling current minima for a fixed bias voltage occur at  $\hbar\omega_c = E_F/n$  ( $n=1,2,\dots$ ). Hickmott<sup>2</sup> associates the current maxima with the condition  $(n+1/2)\hbar\omega_c = E_F$  ( $n=0,1,\dots$ ) and the current minima with the condition  $n\hbar\omega_c = E_F$  ( $n=1,2,\dots$ ). From Fig. 5, it is clear that the tunneling current extremum points does not coincide with the positions predicted by these conditions. This indicates that we can use the expression  $E_F/(n+\phi)$  with both  $E_F$  and  $\phi$  as adjustable parameters to fit the experimental results and obtain an estimate of the zero-field Fermi energy (equal to the value of  $E_F$ ). The positions of the minimum and maximum points of the tunneling current obtained in our theoretical calculation are listed in Tables I and Tables II, respectively. We can accurately fit these extremum positions with  $\phi=0.19$ ,  $\phi=0.86$ , as it is shown in these tables that the extremum positions calculated using the expression  $E_F/(n+\phi)$  with corresponding values of  $\phi$  are very close to the results obtained by the variational method. Our results here indicate that the empirical models used in Eaves *et al.*<sup>1</sup> and Hickmott,<sup>2</sup> which use  $\phi=0$  for minima and  $\phi=1/2$  for maxima, only provide an approximate fit to the experimental results.

#### D. Magnetocapacitance

There have been some measurements of the magnetocapacitance of 2DEG's in GaAs/(AlGa)As modulation-doped heterostructures<sup>11,12</sup> and tunneling heterostructures,<sup>3</sup> which have been used to extract the density of states under magnetic fields. Some analyses of the experimental results<sup>11,12</sup> have been based on the following equation:

$$\frac{1}{C} = \frac{b}{\epsilon_r \epsilon_0} + \frac{\gamma \langle z \rangle}{\epsilon_r \epsilon_0} + \frac{1}{e^2} \frac{dn}{dE_F}, \quad (18)$$

where  $\gamma$  is a numerical constant (0.5–0.7),  $\langle z \rangle$  is the average distance of the charges from the barrier, and  $dn/dE_F$  is the thermodynamic density of states. Assuming the charge den-

TABLE II. Positions of current maximum.

	Current maximum obtained from Fig. 5	Current maxima predicted by $E_F/(n+\phi)$ with $\phi=0.86$ and $E_F=17.8$ meV
$n=0$	20.66 meV	20.69 meV
$n=1$	9.5 meV	9.56 meV
$n=2$	6.19 meV	6.22 meV
$n=3$	4.54 meV	4.61 meV

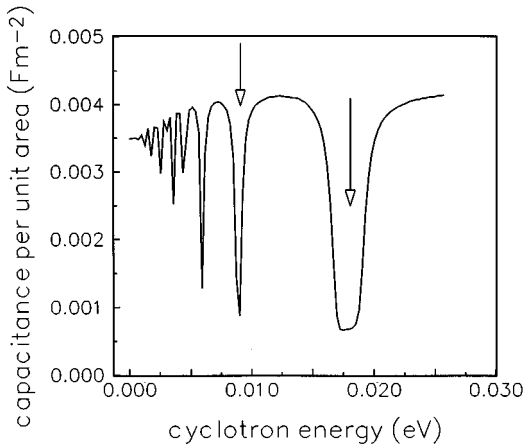


FIG. 7. The differential capacitance per unit area plotted as a function of the cyclotron energy. The arrows show the positions for  $n\hbar\omega_c = E_F$ , where  $n = 1, 2$ .

sity,  $b$  and  $\langle z \rangle$  are constants, the density of states can be easily extracted from the measured capacitance by fitting the experimental results to Eq. (18). These results are very useful as it can be used to investigate the scattering of electrons under a magnetic field. As discussed above, in a tunneling heterostructure, the magnetic field can modify the potential profile in the heterostructure,  $\langle z \rangle$ , and the 2DEG charge density. It is therefore interesting to study how the magnetocapacitance is affected by the changes in these quantities.

The differential capacitance per unit area  $C = dQ/dV$  is calculated by changing the bias by a small amount  $\delta V$  and then determining the ratio between the change in the charge density  $\delta Q$  and  $\delta V$ . When the charge density is changed it is usually accompanied by a change in the potential profile throughout the heterostructure and a shift in the bound-state energy. As a result the small change in the external applied voltage is not equal to the change in the Fermi energy of the 2DEG. From Fig. 1, the relation between  $\delta V$  and  $\delta E_F$  is given as

$$e\delta V = \delta E_F + \delta E_B, \quad (19)$$

where  $\delta E_B$  is the change in the bound-state energy. Hence, the relation between capacitance  $C$  measured and the density of states  $dN/dE_F$  is given by

$$\frac{1}{C} = \frac{1}{e^2 \frac{dN}{dE_F}} + \frac{1}{e^2 \frac{dN}{dE_B}} = \frac{1}{C_q} + \frac{1}{C_b} + \frac{b}{\epsilon_r \epsilon_0}, \quad (20)$$

where  $C_q = e^2(dN/dE_F)$  is called the quantum capacitance<sup>16</sup> and  $C_b$  is the capacitance due to modulation of the bound-state energy relative to the band edge. The applied magnetic field can modulate both  $C_b$  and  $C_q$  and hence it is necessary to estimate the contribution of  $C_b$  to  $C$ .

We have determined the capacitance from the results of our numerical calculations of 2DEG charge as a function of bias voltage. In Fig. 7,  $C$  is plotted as a function of magnetic field and in Fig. 8 the separate contributions  $C_q$  and  $C_b$  are plotted. It can be seen that  $C$  is a minimum when the density of state at the Fermi level is a minimum and is a maximum when the density of states at the Fermi level is a maximum.

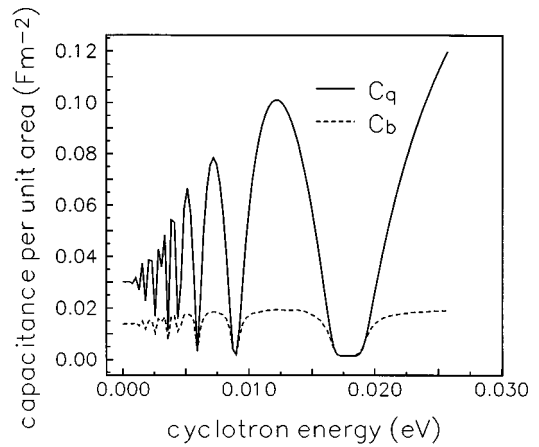


FIG. 8. The areal capacitance  $C_q$  and  $C_b$  plotted as a function of the cyclotron energy.

Qualitatively the measured capacitance agrees with the behavior predicted by Eq. (18) assuming  $\langle z \rangle$  constant. However, in Fig. 8, we show that the change of  $C_b$  with the magnetic field is not negligible. The modulation of  $C_b$  by the magnetic field has to be taken into account, if we want to obtain quantitative information of density of states from the total magnetocapacitance. In Fig. 8, we notice that when the Fermi level is close to a Landau level where the density of states is large,  $C_q$ , proportional to the density of states, is much larger than  $C_b$ . For the parameters used in the present work,  $C_q$  is at least 10 times larger than  $C_b$ . Therefore in this regime, change in  $C$  is mainly determined by  $C_b$ , which is determined by how the bound-state energy responds to the change in the 2DEG charge density. When the Fermi level is in the middle of two Landau levels (i.e., the density of states of the Fermi level is small),  $C_q$  and  $C_b$  are very close in value from Fig. 8. Therefore, the change in  $C$  has two equal contributions from  $C_q$  and  $C_b$ . In this case, if we analyze the magnetocapacitance using Eq. (18), the density of states obtained will be reduced by about 50%. These results demonstrate that it is not accurate to obtain the density of states of a 2DEG in a tunneling heterostructure by fitting the magnetocapacitance with Eq. (18).

## V. CONCLUSION

We have used a simple variational approach to determine the effects of a magnetic field on the accumulation layer in a III-V single barrier tunneling structure. Based on a simple model, we can explain using some physical arguments the modulation mechanism of the charge density and the Fermi level. This provides a framework of understanding for a series of experiments carried out by our group<sup>1</sup> and by Hickmott.<sup>2</sup> We find [considering the InP/(InGa)As heterostructure in the numerical calculation] that the charge distribution in the accumulation layer changes with the magnetic field. As a result, the distance of charges from the barrier, the Fermi energy, and the electron density oscillates with a changing magnetic field. It is not correct to assume either a constant charge density or a constant Fermi energy when the magnetic field is changed. Our calculation shows that the magnetic-field dependence of the tunnel current is mainly the effect of the modulation of the charges' distance from the



barrier and the charge density.

Our model provides a theoretical foundation to the empirical analyses used by Eaves *et al.*<sup>1</sup> and Hickmott.<sup>2</sup> From the results we find that the oscillatory behavior of the current is determined by the position of the Fermi level with respect to the Landau levels. Therefore, from the current oscillations, we can estimate the positions of the Fermi level with respect to the Landau levels. When the current increases with the magnetic field, the Fermi level should be approximately midway between two Landau levels, where the density of states is small. When the current decreases with an increase in magnetic field, the Fermi level is near to a Landau level where there are a high density of states. From the magnetic fields at which the current increases or decreases with field, we can deduce the range of the Fermi energies at these fields. Since the field-dependent Fermi energies oscillates about the zero-field value, this range of values give us an estimate of the zero-field value. If the broadening does not smear out the oscillatory structures, the current minima and maxima occur when the Fermi level is approximately midway between two Landau levels. This suggests that the current minima and maxima can be fitted with the expression  $B_1/(n + \phi)$ , where  $B_1$  and  $\phi$  are adjustable parameters. We fit our numerical results with  $B_1 = 17.8$  meV and  $\phi = 0.19$  and  $0.86$  for current

minima and maxima, respectively, while in Eaves *et al.*<sup>1</sup> and Hickmott<sup>2</sup>  $\phi$  equals to 0. and 0.5 for the minima and maxima, respectively. This explain why the empirical analyses can be used to obtain an estimate of the charge density and Fermi energy at zero magnetic field.

We have also studied the magnetocapacitance of the accumulation layer and show that there is a contribution of the charge rearrangement of the accumulation layer to the capacitance. When charges are added to the 2DEG, the bound state energy is modified as well as the potential profile. This effect contributes to the total capacitance. The change in the bound-state energy depends on the density of states and is thus modulated by the magnetic field. The contribution of this effect to the magnetocapacitance of the 2DEG is not negligible. As a result the effect of the density of states of the 2DEG on the magnetocapacitance has to be determined by some model calculation and cannot be analyzed using the approach used by Weiss, Klitzing, and Mosser.<sup>11</sup>

#### ACKNOWLEDGMENTS

This work was supported in part by the CityU of Hong Kong Strategic Research Grant.

\*Electronic address: apkschan@cityu.edu.hk

<sup>1</sup>L. Eaves, B. R. Snell, D. K. Maude, P. S. S. Guimaraes, D. C. Taylor, F. W. Sheard, and G. A. Toombs, *Proceedings of the 18th International Conference on Physics of Semiconductors, Stockholm* (World Scientific, Singapore, 1986), pp. 1615–1622.

<sup>2</sup>T. W. Hickmott, *Phys. Rev. B* **32**, 6531 (1985).

<sup>3</sup>H. Zheng, A. Song, F. Yang, and Y. Li, *Phys. Rev. B* **49**, 1802 (1994).

<sup>4</sup>J. A. Appelbaum and G. A. Baraff, *Phys. Rev. B* **4**, 1235 (1971).

<sup>5</sup>G. A. Baraff and J. A. Appelbaum, *Phys. Rev. B* **5**, 475 (1972).

<sup>6</sup>U. Ekenberg, *Semicond. Sci. Technol.* **2**, 802 (1987).

<sup>7</sup>J. Sune, P. Olivo, and B. Ricco, *J. Appl. Phys.* **70**, 337 (1991).

<sup>8</sup>G. A. Baraff and D. C. Tsui, *Phys. Rev. B* **24**, 2274 (1981).

<sup>9</sup>J. Sanchez-Dehesa, F. Meseguer, F. Borondo, and J. C. Mean, *Phys. Rev. B* **36**, 50 703 (1987).

<sup>10</sup>K. S. Chan, F. W. Sheard, G. A. Toombs, and L. Eaves, *Superlattices Microstruct.* **9**, 23 (1991).

<sup>11</sup>D. Weiss, K. V. Klitzing, and V. Mosser, *Two-dimensional Systems: Physics and New Devices*, edited by G. Bauer, F. Kuchar, and H. Heinrich, Springer Series in Solid State Science Vol. 67 (Springer-Verlag, Berlin, 1986), pp. 204–217.

<sup>12</sup>V. Mosser, D. Weiss, K. V. Klitzing, K. Ploog, and G. Weimann, *Solid State Commun.* **58**, 5 (1986).

<sup>13</sup>T. P. Smith, B. B. Goldberg, P. J. Stiles, and M. Heiblum, *Phys. Rev. B* **32**, 2696 (1985).

<sup>14</sup>F. W. Sheard and G. A. Toombs, *Appl. Phys. Lett.* **52**, 1228 (1988).

<sup>15</sup>F. Fang and W. E. Howard, *Phys. Rev. Lett.* **16**, 797 (1966).

<sup>16</sup>S. Luryi, *Appl. Phys. Lett.* **52**, 501 (1988).